A global sensitivity analysis approach for marine biogeochemical modeling

Clémentine Prieur, Laurence Viry, Eric Blayo, Jean-Michel Brankart

A global sensitivity analysis approach for marine biogeochemical modeling

C. Prieur[a], L. Viry[a], E. Blayo[a], J.-M Brankart[b]

[a] *Univ. Grenoble Alpes, CNRS, Inria, Grenoble INP*, LJK, 38000 Grenoble, France*
[b] *Univ. Grenoble Alpes, CNRS, Grenoble INP*, IGE, 38000 Grenoble, France*
* *Institute of Engineering Univ. Grenoble Alpes*

Abstract

This paper introduces the Sobol' indices approach for global sensitivity analysis (SA), in the context of marine biogeochemistry. Such an approach is particularly well suited for ocean biogeochemical models, which make use of numerous parameters within large sets of differential equations with complex dependencies. This SA allows for a detailed study of the relative influence of a large number of input parameters on output quantities of interest to be chosen. It is able to distinguish between direct effects of these parameters and effects due to interaction between two or more parameters. Although demanding in terms of computation, such a tool is now becoming affordable, thanks to the development of distributed computing environments. An applicative example is presented with the MODECOGeL biogeochemical model, and illustrates the advantages of this approach over standard local SA.

Keywords: sensitivity analysis, Sobol' indices, marine biogeochemistry

1. Introduction

Marine biogeochemical models are now commonly included as modules in complex ocean circulation modeling systems. They are thus increasingly used for many applications. However, the use of these models raises difficult questions, especially regarding their tuning. They are generally systems of nonlinear ordinary differential equations, with each equation expressing the time evolution of a given state variable due to hydrodynamical effects (transport and diffusion) and to fluxes between the various components of the ecosystem. Two features of these models are noteworthy. First, the evaluation of the fluxes involves a wide variety of processes, and hence numerous

parameters (typically several times more than the number of variables). Secondly, the values of these parameters are often quite poorly known. In reality, the values of the parameters depend on the physical and biogeochemical context, while in practice the available reference values were usually estimated only in a particular situation (e.g. during a field experiment or in laboratory experiments), not in the actual context of interest. The uncertainty of these values is thus generally quite large (see for example Schartau et al. (2017) for a review on the identification of such parameters).

In this context, *sensitivity analysis* (SA), i.e. methods that aim to quantify the relative influence of the inputs on some given outputs in a complex system like a numerical model, are a valuable tool. Indeed, they can help better understand the model itself, and identify which parameters are most influential and should be calibrated carefully. These methods may be divided in two main categories: *local* sensitivity methods that consider the behavior of the solution with respect to small parameter variations and *global* sensitivity methods that determine the behavior of the solution under parameter perturbations of arbitrary magnitude. A common approach is to conduct a few experiments in which the values of parameters vary, either one-at-a-time (OAT), or simultaneously (e.g. Druon and Le Fèvre (1999); Baklouti et al. (2006); Kriest et al. (2012)). Some additional techniques are also sometimes used, such as linear error propagation (Omlin et al., 2001) or the Gaussian emulation machine approach (Scott et al., 2011), which clearly involve global sensitivity analysis.

Another approach defines the sensitivity of the output with regard to the input as the corresponding gradient (both input and output variables must of course be continuous real-valued quantities). This so-called *gradient based SA* thus requires computing gradients. This is straightforward for simple cases, but challenging in general. For instance, the gradient of a single output quantity Q with regard to a constant parameter P can be approximated by $(Q(p+\alpha) - Q(p))/\alpha$, where p is the current value of P and α is taken to be small. The computation of this approximate gradient simply requires running the model twice, using successively p and $p+\alpha$ for parameter P. However estimating the gradient can be much more difficult if P is multivariate or non-constant (e.g. if P is a space and/or time dependent coefficient). In such cases, the preceding approach of computing growth rates requires $N+1$ evaluations of the model, where N is the dimension of P (e.g. the number of space-time grid points). If N is large, an alternative to computing growth rates is to use the so-called *adjoint method*, which provides the exact gradient.

This approach was used for instance in Fennel et al. (2001), Faugeras et al. (2003) and Tjiputra et al. (2007).

However the gradient is computed, it is important to understand that gradient based SA is a local method, in the sense that the gradient is a local notion, computed in the vicinity of the current value of P. Therefore, this gradient, which is a way to quantify the influence of P on Q, can be quite different depending on the value of P chosen. This limitation can be avoided by using an approach based on a global sensitivity measure, i.e. an approach that quantifies the influence of P on Q taking into account the possible variation of P. Such a quantification is provided, for example, by *Sobol' indices*, which will be introduced in the next section. Given their global character, computing such indices may of course require a huge number of model evaluations, which increases with the input space dimension. Therefore it is usual to first carry out, as a preliminary step, a screening analysis, such as the OAT screening approach introduced in Morris (1991). A screening procedure aims at fixing the input parameters whose influence on the output is qualified as negligible after a rough exploration of the input parameter space. It reduces the input space dimension. Then, in a second step, a Monte Carlo sampling-based sensitivity and ranking analysis is run (see, e.g., Sankar et al., 2018) or Sobol' indices are computed (see, e.g., Morris et al., 2014; Wang et al., 2018). However, given the increases in computational resources, we think that performing a direct global SA is now feasible, even for a high-dimensional input space, and that it is time for the scientific community to make computation of Sobol' indices the first choice, particularly when dealing with highly parameterized models.

In this context, the aim of this paper is to introduce the Sobol' indices approach for global sensitivity analysis, and to illustrate its feasibility and its scientific relevance in the context of marine biogeochemistry. Note, however, that our focus is to present the methodological tools in the context of a particular example, rather than to conduct an in-depth physical analysis. First, the global SA approach and the Sobol' indices are introduced in Section 2. Then, in Section 3, we present the biogeochemical model, its many uncertain parameters and the selected output quantities. Section 4 is devoted to implementation aspects of the SA, and Section 5 focuses on results that help illustrate the features of this method. In particular, a comparison with a gradient-based local analysis is presented.

2. Global sensitivity analysis: the framework

As indicated above, the aim of sensitivity analysis is to determine which model inputs are the most influential on some given model outputs. In the following, a model output y is considered to be a deterministic scalar function of some model inputs $\mathbf{x} = (x_1, \ldots, x_d)$, where these inputs belong to a domain Δ:

$$y = y(\mathbf{x}) = y(x_1, \ldots, x_d) \qquad \text{with } \mathbf{x} \in \Delta$$

In Section 3, we consider various scalar outputs, corresponding to different quantities of interest. In this paper, we adopt the stochastic framework of global sensitivity analysis. Unlike local sensitivity analysis, which analyses how a small perturbation near an input space value $x^0 = (x_1^0, \ldots, x_d^0)$ influences the value of the scalar output, global sensitivity analysis considers the whole variation range in the input space. More precisely, each input parameter is considered to be a random variable X_j $(j = 1, \ldots, d)$, where its uncertainty is modeled by some one-dimensional probability distribution. The output Y is then assumed to be a scalar random variable $Y = f(\mathbf{X})$, where $\mathbf{X} = (X_1, \ldots, X_d)$ with the X_i assumed to be independent. Various sensitivity measures have been proposed in the global framework. We focus in this paper on variance-based sensitivity measures, introduced in Sobol' (1993).

2.1. Variance-based sensitivity measures

In order to quantify the influence of the variations of X_j on the variations of Y, let us consider the conditional expectation $\mathrm{E}(Y|X_j = x_j)$. It corresponds to the mean value of Y over the probability distributions of the X_k $(k \neq j)$, when X_j is fixed to x_j. The corresponding random variable, when considering the variations of X_j, is $\mathrm{E}(Y|X_j)$, and its variance quantifies the influence of X_j on the dispersion of Y. The so called Sobol' sensitivity indices are obtained by normalizing this variance by the total variance of the output Y, which is assumed to be finite and non null. Thus the first-order Sobol' sensitivity index of input parameter X_j is defined as

$$\mathrm{S}_{\{j\}} = \frac{\mathrm{Var}\big(\mathrm{E}(Y|X_j)\big)}{\mathrm{Var}(Y)}\,. \tag{1}$$

It belongs to the interval $[0, 1]$.

2.2. The Sobol' decomposition

More generally, starting from the functional Analysis of Variance (ANOVA) decomposition (Hoeffding, 1948; Efron and Stein, 1981; Owen, 1992; Sobol', 1993), one can define sensitivity indices of any order $r \in \{1, \ldots, d\}$. Let us first introduce some notation. We assume that f is a real square integrable function, $\mathfrak{u}$ is a subset of $\{1, \ldots, d\}$, $\mathfrak{u}^c$ stands for its complement, its cardinality is denoted by $r = |\mathfrak{u}|$, and $\mathbf{X}_\mathfrak{u}$ represents the random vector with components X_j, $j \in \mathfrak{u}$. The functional ANOVA decomposition then states that $Y = f(\mathbf{X})$ can be uniquely decomposed into summands of increasing size

$$Y = f(\mathbf{X}) = \sum_{\mathfrak{u} \subseteq \{1,\ldots,d\}} f_\mathfrak{u}(\mathbf{X}_\mathfrak{u}) \tag{2}$$

where $f_\emptyset = \mathbb{E}[Y]$ and the other components have zero mean value and are mutually uncorrelated. This decomposition (2) yields a corresponding decomposition of the variance of the output:

$$\mathrm{Var}(Y) = \sum_{\mathfrak{u} \subseteq \{1,\ldots,d\}, \mathfrak{u} \neq \emptyset} \mathrm{Var}\left(f_\mathfrak{u}(\mathbf{X}_\mathfrak{u})\right) . \tag{3}$$

For any $j \in \{1, \ldots, d\}$, the term $\mathrm{Var}\left(f_{\{j\}}(X_j)\right)$ corresponds to the part of the output variance explained by parameter X_j. For any $j, j' \in \{1, \ldots, d\}$, $j < j'$, the term $\mathrm{Var}\left(f_{\{j,j'\}}(X_j, X_{j'})\right)$ corresponds to the part of the output variance explained by combined effects of parameters X_j and $X_{j'}$. More generally, for any $u \subseteq \{1, \ldots, d\}$, the term $\mathrm{Var}\left(f_\mathfrak{u}(\mathbf{X}_\mathfrak{u})\right)$ corresponds to the part of the output variance explained by combined effects of parameters X_j, $j \in \mathfrak{u}$. Then, for any $\mathfrak{u} \subseteq \{1, \ldots, d\}$, the Sobol' index (Sobol', 1993) of order $r = |\mathfrak{u}|$ associated to the vector $\mathbf{X}_\mathfrak{u}$ is defined as

$$\mathrm{S}_\mathfrak{u} = \frac{\sigma^2_\mathfrak{u}}{\sigma^2} = \frac{\mathrm{Var}\left(f_\mathfrak{u}(\mathbf{X}_\mathfrak{u})\right)}{\mathrm{Var}(Y)} . \tag{4}$$

The main effect of the j^{th} factor is thus measured by $\mathrm{S}_{\{j\}}$. Then the effect due to the specific interaction between the j^{th} and k^{th} factors ($k \neq j$) is measured by $\mathrm{S}_{\{j,k\}}$. And so on for higher order indices (Saltelli et al., 2000). Corresponding cumulative effects are defined by so-called closed Sobol' indices, defined as

$$\mathrm{S}^{\text{closed}}_\mathfrak{u} = \sum_{\mathfrak{v} \subset \mathfrak{u}} \mathrm{S}_\mathfrak{v} . \tag{5}$$

We thus have for instance $S^{\text{closed}}_{\{j,k\}} = S_{\{j\}} + S_{\{k\}} + S_{\{j,k\}}$, which means that the closed second-order index $S^{\text{closed}}_{\{j,k\}}$ measures the effect of the interactions between parameters X_j and X_k in addition to the main effect of each of these two parameters.

For any $j \in \{1, \ldots, d\}$, we also define a total sensitivity index $S^{\text{tot}}_{\{j\}}$ (Homma and Saltelli, 1996) to express the overall sensitivity to an input X_j as

$$S^{\text{tot}}_{\{j\}} = \sum_{\mathfrak{v} \subset \{1,\ldots d\} \text{ with } j \in \mathfrak{v}} S_{\mathfrak{v}} \,. \tag{6}$$

We have then, for instance, in the case where $d = 3$: $S^{\text{tot}}_{\{1\}} = S_{\{1\}} + S_{\{1,2\}} + S_{\{1,3\}} + S_{\{1,2,3\}}$.

2.3. Estimating the Sobol' indices

For simple models, sensitivity analysis can sometimes be done analytically, by direct examination of their mathematical expression. However, this is of course generally not the case for complex models. In those cases, one evaluates the model for selected values of the input parameters, and the resulting output values are used to estimate sensitivity indices of interest. For interested readers, Monte Carlo based procedures for the estimation of Sobol' indices are described in detail in Appendix A.

Let us summarize the different strategies we apply in Section 5:

- In Subsection 5.1, we apply the replication procedure introduced in Mara and Rakoto Joseph (2008) (and further studied in Tissot and Prieur (2015)) to estimate all first-order Sobol' indices with only two replicated d-dimensional Latin hypercube samples of size n, that is with only $2n$ model evaluations.

- In Subsection 5.2, we apply the replication procedure introduced in Tissot and Prieur (2015) to estimate all closed second-order Sobol' indices with only two replicated d-dimensional randomized orthogonal arrays of strength 2 and size n, that is again with only $2n$ model evaluations. Due to constraints in the construction of orthogonal arrays of strength 2, n must be chosen as q^2, with q a prime number greater than, or equal to, $d - 1$.

- In Subsection 5.3, we apply the procedure introduced in (Saltelli, 2002, Theorem 1) to estimate all first-order and total Sobol' indices with a

cost of only $(d+2)n$ model evaluations. This procedure is based on combinatorial arguments.

These procedures are implemented in the functions `sobolroalhs`, `sobolSalt` of the package `sensitivity`. All these strategies are detailed in Appendix A. A crucial point in the above summary is that the cost (in terms of number of model evaluations) required to estimate total Sobol' indices is only linear in the input space dimension d. In the following (see Section 4), we present an implementation using a grid computing environment. However, even in such a framework, the estimation of total Sobol' indices be expensive if d is large. Thus, depending on the computational resources of the study, one could avoid the estimation of these total indices and focus instead on the estimation of all first-order and closed second-order Sobol' indices as a first step in the sensitivity analysis.

3. Description of the ocean biogeochemical model

The SA approach is applied to the 1D biogeochemical MODECOGeL model of the ocean mixed layer described in subsection 3.1. The uncertain input parameters of the model (vector $\mathbf{x}$ in Section 2) are described in subsection 3.2 and several output quantities (y in Section 2) are listed in subsection 3.3, corresponding to key model results whose sensitivity to the input parameters is not obvious.

3.1. The MODECOGeL model

The model used in this paper is MODECOGeL[1]. It was developed for investigating the biogeochemical activity in the Ligurian sea by Lacroix (1998) by coupling a 1D hydrodynamic model of the mixed layer to a 12-component ecosystem model.

The hydrodynamic model is a 1D version of the GHER primitive equations model (Nihoul and Djenidi, 1987). The state variables are the horizontal velocity, the potential temperature, the salinity, and the turbulent kinetic energy. A full description of the model can be found in Lacroix and Nival (1998) or Lacroix and Grégoire (2002), where it is applied to simulate the behavior of the system during the FRONTAL oceanographic campaigns from

[1]MODECOGeL: MODèle d'ECOsystème du GHER (GeoHydrodynamics and Environment Research) et du LOV (Laboratoire d'Océanographie de Villefranche-sur-Mer)

1984 to 1988. In the present paper, the model is applied to years 2006–2007, and the atmospheric dataset is extracted mainly from the Côte d'Azur meteorological buoy located at the DYFAMED station (BOUSSOLE project) at hourly frequency (Marty and Chiavérini, 2010).

The ecosystem model provides a 12-component description of the ecosystem of the Ligurian Sea (see state variables in Table 1). A detailed description of this model can be found in Lacroix and Grégoire (2002). The time evolution of each state variable is governed by the equation:

$$\frac{\partial C_i}{\partial t} = \mathtt{ADV}_i + \mathtt{DIFF}_i + \mathtt{SMS}_i \quad \text{with} \quad \mathtt{SMS}_i = \sum_{j \neq i} \mathtt{FLUX}(C_j \rightarrow C_i) \qquad (7)$$

where $\mathtt{ADV}_i$ and $\mathtt{DIFF}_i$ are advection and diffusion terms (governed by the hydrodynamic model), and $\mathtt{SMS}_i$ is the "source minus sink" term summing up the fluxes ($\mathtt{FLUX}(C_j \rightarrow C_i)$) between the various components of the ecosystem (conservation of course imposes that $\mathtt{FLUX}(C_j \rightarrow C_i) = -\mathtt{FLUX}(C_i \rightarrow C_j)$). These fluxes can be sorted into several categories: primary production, secondary production, mortality, exudation, excretion, growth of bacteria, decomposition of particulate organic matter, and nitrification. We refer to Appendix B for a detailed description of these different processes.

Equation (7) is solved numerically between the sea surface and 405 m depth using a constant vertical discretization (1 m) and a constant time step (6 minutes). Outputs are saved daily at all depths.

It is important to note that the mathematical expression of these flux terms contains numerous parameters whose values are not known precisely. In the following, consistent with the objective of this study, we provide only a brief overview of these model parameters, with a specific focus on the assumptions that we make regarding their respective uncertainties.

3.2. Model parameters

The biogeochemical fluxes ($C_j \rightarrow C_i$) parameterized in MODECOGeL are summarized in Table B.8 (Appendix B). Each flux depends on several of the parameters listed in Table C.9 (Appendix C). Moreover, the parameterization of each process as a joint function of the model state and parameters is often complex and nonlinear. As a result, it is usually impossible for the user to know the sensitivity of the whole system to the parameters. A systematic computational approach is thus needed.

Variable	Acronym	Name
C_1	**NO3**	Nitrate
C_2	**NH4**	Ammonium
C_3	**PicP**	Picophytoplankton
C_4	**NanP**	Nanophytoplankton
C_5	**MicP**	Microphytoplankton
C_6	**NanZ**	Nanozooplankton
C_7	**MicZ**	Microzooplankton
C_8	**MesZ**	Mesozooplankton
C_9	**BAC**	Bacteria
C_{10}	**DON**	Dissolved organic nitrogen
C_{11}	**POM1**	Particulate organic matter (size 1)
C_{12}	**POM2**	Particulate organic matter (size 2)

Table 1: Model state variables.

To apply the SA method described in Section 2, a probability distribution must be specified for each input parameter. This has been done here using the following guidelines:

- In the absence of any reliable information about possible correlations, the uncertainties of the various parameters are assumed independent.
- Most parameters are constrained to be either positive or negative, for consistency with the formulations used to parameterize the processes. They are assumed to follow a Gamma distribution.
- Parameters constrained between 0 and 1 are assumed to follow a Beta distribution.
- Some parameters are constrained to be larger than 1. Their logarithm is assumed to follow a Gamma distribution.
- Some parameters are not constrained, and are assumed to follow a Gaussian distribution.
- Three different values for standard deviations are used (5%, 20%, 50% of the expected value) according to the confidence we have in the parameters. These values were provided by biogeochemical modelers using a priori knowledge.

The resulting probability distributions are given in Table C.9 (Appendix C).

3.3. Quantities of interest

The quantities of interest (QoI), i.e. the output values y, must be defined according to the main scientific objectives of the sensitivity study. In the present case, for this example, we have chosen to focus on characterizing the simulation of phytoplankton (concentrations C_3, C_4, C_5 in Table 1), which is at the base of the marine food web. As an additional quantity, we also introduce chlorophyll concentration (noted C_0), which is what is observed by ocean color data, and which can be approximately computed from phytoplankton concentrations using a constant chlorophyll to nitrogen ratio (α):

$$C_0 = \alpha(C_3 + C_4 + C_5) \tag{8}$$

Since sensitivity analysis applies to scalar output quantities, to apply the SA method we need to reduce the time and space variations of C_0, C_3, C_4, C_5 to some scalar indicators. Note that the cost of the method is almost independent of the number of these indicators. However, they must be defined before running the sensitivity study. To illustrate the method, we thus decided to introduce a range of different QoI characterizing C_0, C_3, C_4, C_5, without limiting our choice to simple linear diagnostics.

Table 2 summarizes the QoI Y_{ij} that we will use in our application. The second index j corresponds to the computed diagnostic while the first index i corresponds to the concentration ($i = 0, 3, 4, 5$) to which it is applied. This set of five diagnostics is meant to characterize (i) the maximum intensity of the phytoplankton spring bloom, (at the surface and as a vertical average), (ii) the time at which it occurs, and (iii) the overall average over the whole simulation.

4. Practical aspects of the sensitivity analysis

In this section we provide more details about the numerical implementation of the sensitivity analysis, i.e. the computation of estimates of all first, closed second-order and total Sobol' indices.

4.1. Grid computing environment

In most cases, the primary cost of the global sensitivity analysis is due to the need for numerous evaluations of the model. In our study each model

Index j	Diagnostic	Definition
1	surface maximum	$\max_t C_i(0,t)$
2	time of surface maximum	$\mathrm{argmax}_t C_i(0,t)$
3	maximum of vertical average	$\max_t \frac{1}{Z}\int_0^Z C_i(z,t)\,dz$
4	time of maximum of vertical average	$\mathrm{argmax}_t \frac{1}{Z}\int_0^Z C_i(z,t)\,dz$
5	time and vertical average	$\frac{1}{ZT}\int_0^T\int_0^Z C_i(z,t)\,dz\,dt$

Table 2: Quantities of interest Y_{ij}. The maximum depth for averaging is $Z = 40\,\mathrm{m}$ and T is the total duration of the experiment.

evaluation is short (approximately 50s). However, $2n$ evaluations are required to estimate all first-order or all closed second-order Sobol' indices, and $(d+2)n$ evaluations are required to estimate all total Sobol' indices, where n is typically of order $10^3 - 10^6$. Furthermore, we must manage the model's input and output files. This problem thus requires specific tools to automatically organize data management and access to computational resources. Note also that, since we have to perform a very large number of model runs, our computing environment must include fault tolerance.

A grid computing environment (i.e. a distributed architecture of computers linked by communication networks and managed by "middleware" software) is particularly well suited for this kind of application, in which multiple parallel computations take place independently without the need to communicate intermediate results between processors. In our implementation we used computing resources at the University of Grenoble[2], distributed on three sites (10 clusters, 6600 CPU cores and 176 GPU cores). These resources are connected by a local grid[3] associated with several storage nodes distributed among the three sites as close as possible to each supercomputer, and managed by the middleware iRods[4]. Each cluster uses the local resource manager OAR[5] and accesses the full 6600 CPU cores through the middle-

[2]see https://ciment.ujf-grenoble.fr/wiki-pub/index.php

[3]https://ciment.ujf-grenoble.fr/wiki-pub/index.php/Grid_computing

[4]see irods.org

[5]see oar.imag.fr

ware CIGRI[6] which launches embarrassingly parallel jobs on idle processors. CIGRI is able to manage job failures in a smart way, which allows the user to submit many small jobs. As a final step, we also need to transfer many input and result files distributed over different iRods resources on a laptop or a computer server of a laboratory. This is achieved efficiently using a python script.

4.2. Implementation of our study

As indicated above, the MODECOGeL model presented in Section 3 includes 74 uncertain input parameters, each with an associated probability distribution (see Table C.9). The global sensitivity analysis is done with the R package `sensitivity` (Pujol et al., 2017) (R[7] is a free software environment for statistical computing and graphics).

The design of the experiments (DoE) and the estimation of the Sobol' indices and their associated confidence intervals use the functions `sobolroalhs` and `sobolSalt`. Function `sobolroalhs`, which estimates all first-order and all closed second-order indices, is based on the replication procedure briefly described in Subsection 2.3 and detailed in Appendix A. It makes use of four replicated designs of size n (two for first-order indices and two for closed second-order indices).

The grid deployment used for the estimation of all first-order Sobol' indices is done as follows (see also Figure 1):

- Construct two replicated Latin Hypercube Samplings (LHS) of size n with the `sobolroalhs` function.

- Evaluate the model on the DoE. In order to minimize the overhead corresponding to the submission of each evaluation and to optimize the use of the "best effort" mode of the batch manager, the model runs are performed one hundred at a time. Each group of simulations corresponds to 100 different sets of the 74 input parameters, and requires an average cpu time of 84 minutes and a small input and output files of approximately 200Ko. For $n = 10^6$, we thus submitted 20 000 jobs on the computing grid.

[6] http://ciment.ujf-grenoble.fr/cigri/dokuwiki/doku.php
[7] http://cran.r-project.org

- Merge the $2n$ files containing the evaluations of the quantities of interest on the DoE.
- Treat outliers. A small percentage of the model evaluations fail or lead to completely spurious results, due to unrealistic combinations of the input parameters. The quantities of interest are then set to NaN and will be treated as missing values in the computation of Sobol' indices.
- Compute Sobol' indices using the function `sobolroalhs`.

Note that the experimental designs and the functions used to compute Sobol' indices differ for the estimations of closed second-order and total indices, as detailed in Section 2.3.

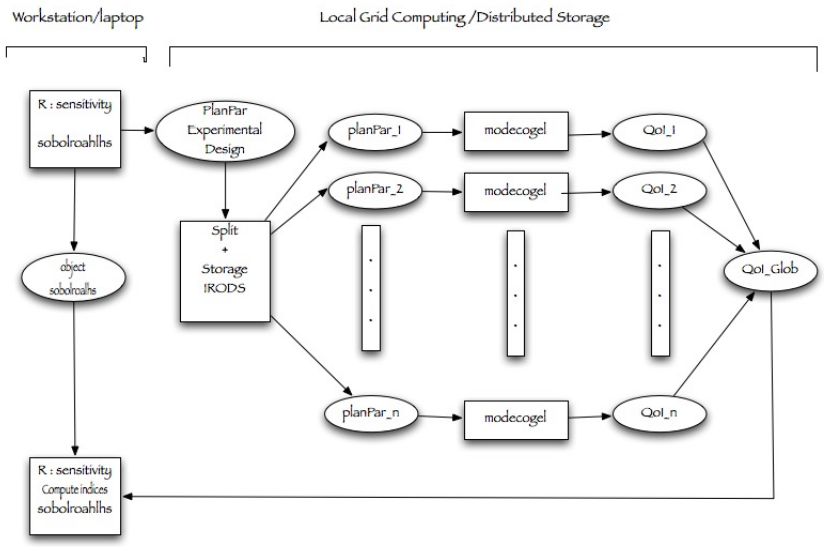

Figure 1: The steps for the estimation of all first-order (or all closed second-order) Sobol' indices with the `sobolroalhs` function of the R `sensitivity` package. The experimental design PlanPar is split into p sets of simulations (100 simulations each in our case). Each set of simulations is performed using MODECOGeL and the QoI are computed for each simulation. All values for the QoI are grouped in a single file QoIGlob, which is sent to `sobolroalhs` for the actual computation of the Sobol' indices.

5. Results

We focus here on the quantities of interest (QoI) which are summarized in Table 3 and described in Section 3. Once again, our aim with this global sensitivity analysis of the MODECOGeL model is not to perform an in-depth biogeochemical analysis of the results (this is outside the scope of this study), but rather to show how these statistical tools provide a better understanding of complex systems involving many parameters.

Quantity of interest	Y_{ij}	Description
maxc	Y_{01}	annual maximum of surface chlorophyll concentration
timechl	Y_{02}	time of maximum of surface chlorophyll concentration
moyc	Y_{05}	time and vertical average of chlorophyll concentration
maxpp	Y_{31}	maximum of surface picophytoplankton concentration
timepp	Y_{32}	time of maximum of surface picophytoplankton concentration
maxmoypp	Y_{33}	maximum of vertical average of picophytoplankton concentration
timemoypp	Y_{34}	time of maximum of vertical average of picophytoplankton concentration
maxnp	Y_{41}	surface maximum of nanophytoplankton concentration
timenp	Y_{42}	time of maximum of surface nanophytoplankton concentration
maxmoynp	Y_{43}	maximum of vertical average of nanophytoplankton concentration
timemoynp	Y_{44}	time of maximum of vertical average of nanophytoplankton concentration
moynp	Y_{45}	time and vertical average of nanophytoplankton concentration

Table 3: Quantities of interest analyzed in the present work. See also §3.3 and Table 2 for the explanation of the notation Y_{ij}

5.1. First-order indices

The 74 first-order Sobol' indices were estimated for each QoI for different values of the sample size: $n = 10^3, 10^4, 10^5, 10^6$. For each index and each value of n, both its estimate and a 95% confidence interval are provided. These results are plotted on Figure 2 for output Y_{01}, namely the maximum surface chlorophyll concentration. As expected, the size of the 95% confidence interval decreases to zero as n increases, and $n = 10^6$ seems to be a sufficiently large sample size to get accurate estimates (size of the 95% confidence interval smaller than 0.01), which allows a clear ranking of the largest indices.

Only ten parameters have a first-order index greater than 0.01 (their values are reported in Table 4). Quite similar results are actually obtained for the other QoIs, and it appears that only 15 or 9 model parameters have a first-order Sobol' index greater than 0.01 for at least 1 or 6 QoIs, respectively (the

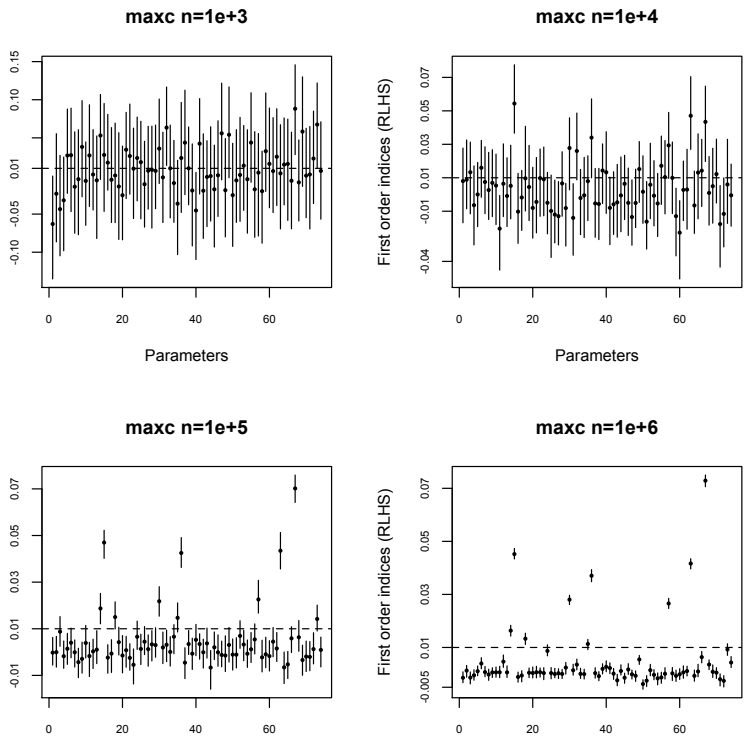

Figure 2: Estimated first-order indices (y-axis) with their 95% confidence interval for the 74 model parameters (x-axis), for $n = 10^3, 10^4, 10^5$ and 10^6, in the case of the output Y_{01}. The dashed horizontal line corresponds to a threshold arbitrarily chosen to be 0.01. Confidence intervals were obtained with a bootstrap procedure (e.g. Archer et al. (1997)) and a bootstrap sample size of 100. Note that Sobol' estimates are not constrained to be positive, which explains that parts of confidence intervals may be below 0.

threshold 0.01 was chosen to guarantee a clear separation between inputs with high and low first-order indices). This is summarized in Figure 3, where these most influential model parameters are clearly visible. This mostly highlights the important sensitivity of our QoIs to the parameterization of excretion for bacteria, of grazing and ingestion for mesozooplankton, and of the variation of light limitation for phytoplankton.

This small number of influential parameters may indicate that an efficient reduction of this model could be performed to produce a reduced order model involving many fewer parameters. Note however that the sum of first-order indices is equal to 0.371. This is far less than 1, which clearly

indicates that the outputs considered are not simple additive models of the form $Y = f_1(X_1) + \ldots + f_d(X_d)$. There are some interaction effects of the parameters on the QoIs, which motivates the investigation of second-order interaction effects.

parameter number (see Table C.9)	67	15	63	36	30	57	14	18	35
estimated index	0.0729	0.0452	0.0416	0.0370	0.0280	0.0266	0.0163	0.0133	0.0113
estimated error	0.0022	0.0020	0.0019	0.0023	0.0018	0.0019	0.0020	0.0021	0.0019

Table 4: Estimation of first-order Sobol' indices for the output Y_{01} (annual maximum of chlorophyll concentration). The estimated error is the radius (half of the length) of the 95% confidence interval.

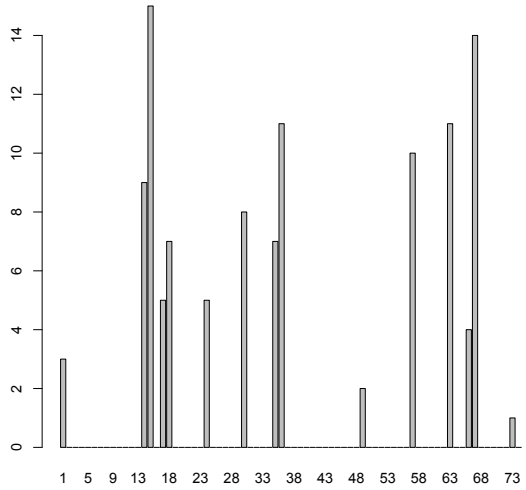

Figure 3: Number of quantities of interest (y-axis) for which the estimate of the first-order index is greater than 0.01. The 15 parameters are: 1 14 15 17 18 24 30 35 36 49 57 63 66 67 73 (x-axis).

5.2. Second order indices

As indicated before, the `sobolroalhs` function allows the estimation of closed second-order indices at a cost of $2n$ model evaluations. Let us recall that the closed second-order index corresponding to the j^{th} and k^{th} parameters is defined as:

$$\mathrm{S}^{\text{closed}}_{\{j,k\}} = \mathrm{S}_{\{j\}} + \mathrm{S}_{\{k\}} + \mathrm{S}_{\{j,k\}} \tag{9}$$

and corresponds to the sum of the main and interaction effects due to these two parameters.

A specificity for the estimation of closed second-order indices with the replication procedure is that n has to be chosen equal to q^2, where $q \geq d-1$ is a prime number denoting the number of levels of the orthogonal array (see Appendix A for more details). A value of $q = 227$, i.e. $2n = 103\,058$, was necessary to achieve sufficiently accurate estimates of the indices.

Estimates of the $d(d-1)/2 = 2701$ closed second-order indices, along with their corresponding 95% bootstrap confidence intervals, were then computed for each QoI. They are displayed in Figure 4 for the output Y_{01} (annual maximum of chlorophyll concentration, which was already chosen in Figure 2 and Table 4). It clearly appears that very few of these 2701 indices are significant. Given the definition (9) of the $\mathrm{S}^{\mathrm{closed}}_{\{j,k\}}$, most of them obviously correspond to at least one influential parameter listed in Table 4, as clearly displayed in Figure 5a.

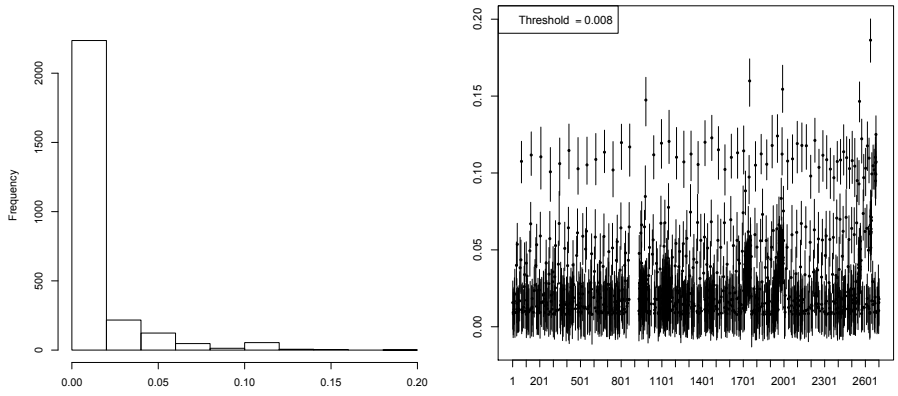

Figure 4: Estimation of second-order closed indices for QoI Y_{01}. Left panel: histogram of the values of the 2701 indices. Right panel: values of these indices with their associated 95% bootstrap confidence intervals (with a bootstrap sample size equal to 100). For sake of clarity, only values greater than 0.008 are shown.

Using these closed second-order index estimates and the previous estimates of first-order index, we compute consistent estimates of unclosed second-order Sobol' indices $\mathrm{S}_{\{j,k\}}$ with a bootstrap algorithm. These indices quantify the fraction of variance of the QoI due to these two parameters that cannot be explained by the sum of the main effect of X_i and X_j, but

only by their interaction. They are displayed in Figure 5b in the particular case of output Y_{01}. New interesting information arises from this plot. First, it appears that input parameters with strong direct influence (i.e. strong first order indices) may or may not have significant interactions with other parameters. For instance, parameters 36 and 57 (see Table C.9), related to semi-saturation for ingestion by MesZ, and fraction of grazing used for growth of MesZ, have weak second order indices. Conversely, parameters 15 and 18, related to variation of light limitation for NanP and to optimal temperature for NanP, which already correspond to large first order indices, have also strong interactions with many other parameters (see Figure 6a). Secondly, some other parameters that have not been noticed yet, since they have weak first order indices, show strong interactions with numerous other parameters. Let us mention in particular parameters 8 and 12, related to NH4 semisaturation for PicP and to optimal PAR for NanP (see Figure 6b). These results are summarized in Figure 6 (recall that the value 0.01 for the threshold in Figure 6 was chosen to guarantee a clear separation between inputs with high and small first-order indices).

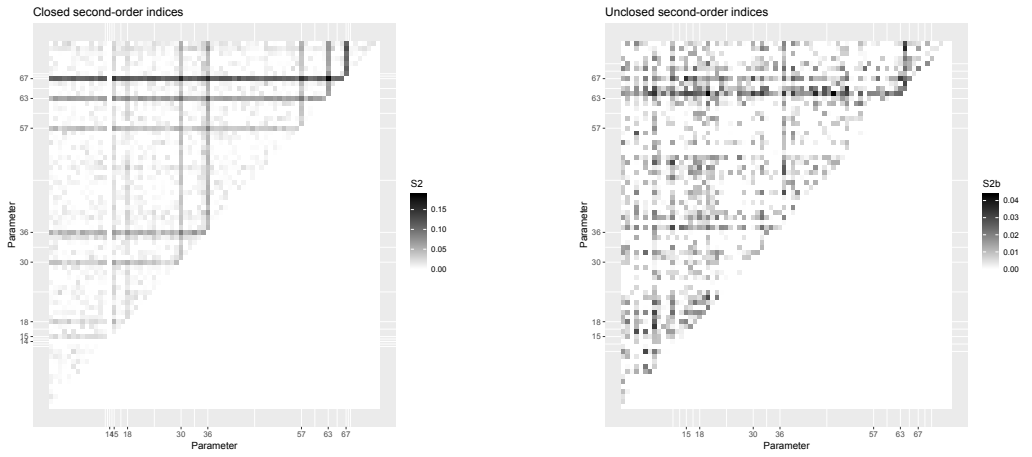

(a) Second-order closed indices $S^{closed}_{\{j,k\}}$ (b) Second-order unclosed indices $S_{\{j,k\}}$

Figure 5: Maps (74×74) of the second-order closed and unclosed Sobol indices for QoI Y_{01}. The x and y axes correspond to the number of the parameters, and the grey scale to the value of the index. Note that the numbers indicated on the axes correspond to parameters with high first-order indices.

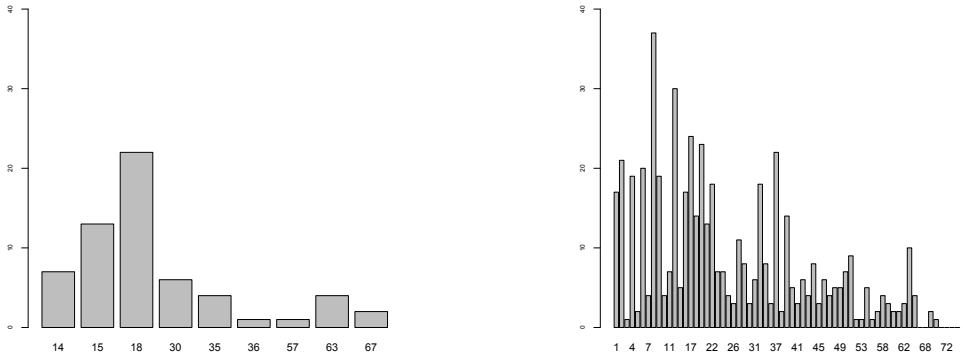

(a) $S_{\{j\}} \geq 0.01$ (b) $S_{\{j\}} \leq 0.01$

Figure 6: Numbers of second-order unclosed indices $S_{\{j,k\}}$ $(j \neq k)$ greater than 0.008, as a function of j, for QoI Y_{01}. Left panel: input parameters with large first-order indices $(S_{\{j\}} \geq 0.01)$. Right panel: input parameters with weak first-order indices $(S_{\{j\}} < 0.01)$.

At this stage, the information from the first- and second-order indices remains incomplete. Higher order interactions can be expected, especially for highly parameterized models like marine biogeochemistry. A natural step forward in the study is then to compute total indices.

5.3. Total order indices

The total Sobol' index $\mathrm{S}^{\mathrm{tot}}_{\{j\}}$ $(j \in \{1, ..., d\})$ defined in Equation (6), expresses the overall sensitivity of some QoI to the input X_j. As mentioned in Section 2 and Appendix A, a competitive procedure to estimate simultaneously all first and total Sobol' indices was introduced in Saltelli (2002) and implemented by the function `sobolSalt` of the R package `sensitivity`. Its cost is, however, still quite high since it requires $(d+2)n$ model evaluations. However, this linear computational complexity with regard to the input space dimension d cannot be avoided. Therefore, depending on the computational resources available for the study, computing such indices is not always affordable, although they bring important information since input parameters with a very low value for their total Sobol' index can be fixed to a nominal value in a calibration procedure.

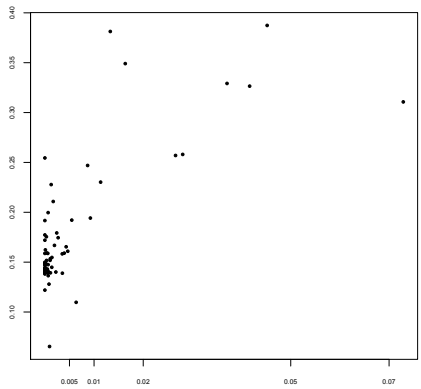

Figure 7: Scatterplot of first-order (x-axis) and total (y-axis) Sobol' indices for output Y_{01}. Note that, for sake of readability, the x-axis is stretched with regard to the y-axis.

A scatter plot of first-order and total indices is displayed in Figure 7. We observe that the parameters contribute to the total variance primarily through their interactions with other parameters (the dots are far above the line $y = x$). However, the relation between first-order and total indices is not linear. More precisely, parameters having a large main effect generally also contribute to the total variance through their interactions with other parameters (Figure 8a). Nevertheless, the relative importance of these interactions may vary significantly. For instance, parameter 67 (temperature variation of excretion for bacteria), which corresponds to the largest first-order index, has a total index smaller than several other parameters with much smaller first-order indices. On the other hand, some parameters with a very small main effect make a non-negligible contribution to the total variance via their interactions with other parameters (Figure 8b). This heterogeneous distribution of the relative importance of the first-order effect with regard to the total effect is summarized in Figure 9, where the ratio $\mathrm{S}_{\{j\}}/\mathrm{S}^{\mathrm{tot}}_{\{j\}}$ is displayed.

5.4. Comparison with a local analysis

The majority of previous sensitivity analyses performed on ocean biogeochemistry models have used local methods, such as the gradient method or methods where parameters are varied one-at-a-time. It is therefore interesting to compare the results we have just obtained using the global Sobol' indices method with equivalent results obtained using local methods applied

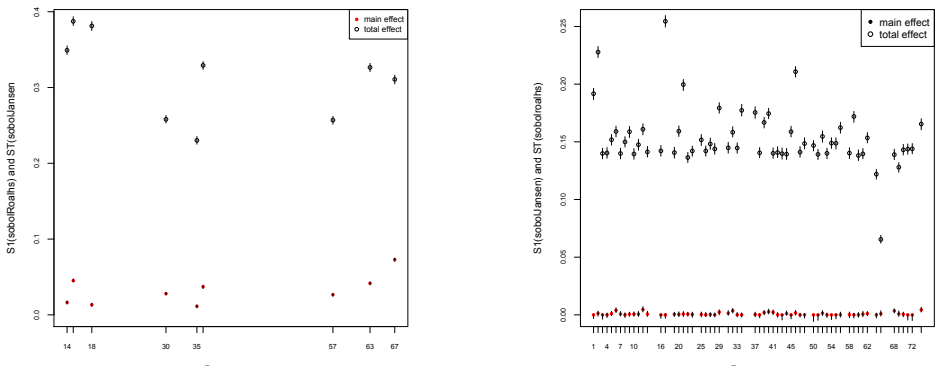

(a) $S_{\{j\}} \geq 0.01$ (b) $S_{\{j\}} \leq 0.005$

Figure 8: y-axis: values of the first-order and total Sobol' indices for the 74 parameters (x-axis), and corresponding confidence intervals, for output Y_{01}. Left panel: parameters with first-order index larger than 0.01 only. Right panel: parameters with first-order index smaller than 0.005 only.

to the same MODECOGeL model.

We have thus computed the gradients of our QoI with regard to the 74 input parameters. The partial derivatives are approximated by

$$\frac{\partial Y}{\partial X_j}(x_1, \ldots, x_d) \simeq \frac{Y(x_1, \ldots, x_{j-1}, x_j + \alpha, x_{j+1}, \ldots, x_d) - Y(x_1, \ldots, x_d)}{\alpha} \tag{10}$$

where α is a small value ensuring very good accuracy of the estimate (in our case, we checked that any value of α between $10^{-3}\sqrt{\mathrm{Var}(X_j)}$ and $10^{-6}\sqrt{\mathrm{Var}(X_j)}$ is relevant and leads to the same value for the gradient). $d + 1$ (i.e. 75 in our case) model runs are required. The local character of this gradient appears clearly in (10): the gradient is computed for a particular value $(X_1, \ldots, X_d) = (x_1, \ldots, x_d)$. In our case, we choose to compute it for the mean values of the 74 parameters (listed in Table C.9), i.e. for $(x_1, \ldots, x_d) = (\mathrm{E}(X_1), \ldots, \mathrm{E}(X_d))$.

As can be seen in Figure 10a and in Table 5, according to this gradient, the two parameters 67 and 66 (temperature variation of excretion for bacteria and mesozooplankton respectively) have a very strong impact on Y_{01}. The importance of parameter 67 was already noted previously, since it corresponds to the largest first-order Sobol' index, and to one of the largest total indices. However, parameter 66 does not appear as one of the most influen-

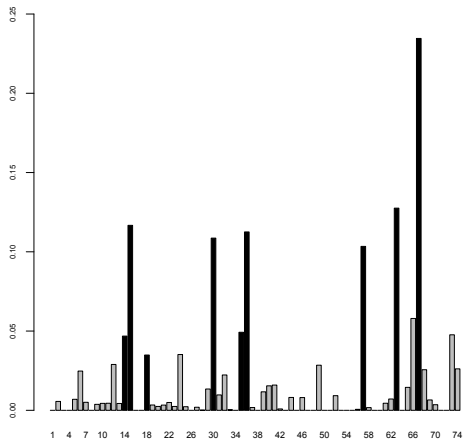

Figure 9: Estimation of the ratio $S_{\{j\}}/S^{tot}_{\{j\}}$ (y-axis) for $j = 1, \ldots, 74$ (x-axis). Black bars correspond to parameters with first-order index larger than 0.01.

tial parameters from the global SA: its ranking is just 12th among first-order indices, and 73rd of 74 considering total indices. Conversely several parameters that were clearly highlighted by the global SA do not correspond to large values of the derivative. This is the case, for instance, for parameter 14 (variation of light limitation for picophytoplankton): its ranking is 3rd considering total indices and 7th considering first-order indices, but only 21st considering derivatives. Similar remarks can be made for parameters 30, 36 and 57 (see Table 6). In the same way, the local analysis indicates that parameters 15 and 18 (variation of light limitation and optimal temperature for nanophytoplankton) are ten times less important than parameters 66 and 67. In contrast, the total Sobol' indices show that they are actually more important (Table 5).

In summary, the local analysis identifies parameters 66 and 67 as important, and only to a much lesser extent a few others. However, the comparison with Sobol' indices clearly shows that this is only local information. Relying only on this local information would lead us to waste effort tuning some parameters and to neglect entirely other important ones.

A complementary way to look at this local gradient is to compute

$$S^{loc}_{\{j\}} = \frac{\mathrm{Var}(X_j)}{\mathrm{Var}(Y)} \left(\frac{\partial Y}{\partial X_j} \right)^2$$

This local index is non dimensional. It can be interpreted as a "relative gradi-

j	67	66	15	18	63	46
$\partial Y/\partial X_j$	3.02	2.17	0.30	-0.28	0.20	-0.20
$\mathrm{S}_{\{j\}}$	0.073	0.006	0.045	0.013	0.042	0.002
$\mathrm{S}^{\mathrm{tot}}_{\{j\}}$	0.311	0.110	0.387	0.381	0.326	0.211

Table 5: Largest values of the local derivative $\partial Y/\partial X_j$ and corresponding first-order and total Sobol' indices $\mathrm{S}_{\{j\}}$ and $\mathrm{S}^{\mathrm{tot}}_{\{j\}}$

j	2	14	15	18	30	35	36	46	57	63	66	67
$\partial Y/\partial X_j$	8^{th}		3^{rd}	4^{th}		7^{th}		6^{th}		5^{th}	2^{nd}	1^{st}
$\mathrm{S}_{\{j\}}$		7^{th}	2^{nd}	8^{th}	5^{th}		4^{th}		6^{th}	3^{rd}		1^{st}
$\mathrm{S}^{\mathrm{tot}}_{\{j\}}$		3^{rd}	1^{st}	2^{nd}	7^{th}		4^{th}		8^{th}	5^{th}		6^{th}

Table 6: Top eight ranking of the local derivative $\partial Y/\partial X_j$, and first-order and total Sobol' indices $\mathrm{S}_{\{j\}}$ and $\mathrm{S}^{\mathrm{tot}}_{\{j\}}$

ent", since it could also be written as $\left(\partial Y'/\partial X'_j\right)^2$, where $Y' = Y/\sqrt{\mathrm{Var}(Y)}$ and $X'_j = X_j/\sqrt{\mathrm{Var}(X_j)}$ are normalized versions of Y and X_j. Its interest for our study lies in the fact that, in the case of a linear dependency $Y = a_0 + a_1 X_1 + \ldots + a_d X_d$ and of the independence of input parameters, this index is equal to the first order Sobol' index. As can be seen in Figure 10b, this index indicates that the most (and almost only) influential parameter is parameter 66 (and, to a much lesser extent, parameter 67). As noted previously, this result is contradicted by the global SA. This disagreement is a clear illustration of the strongly nonlinear character of the MODECOGeL model.

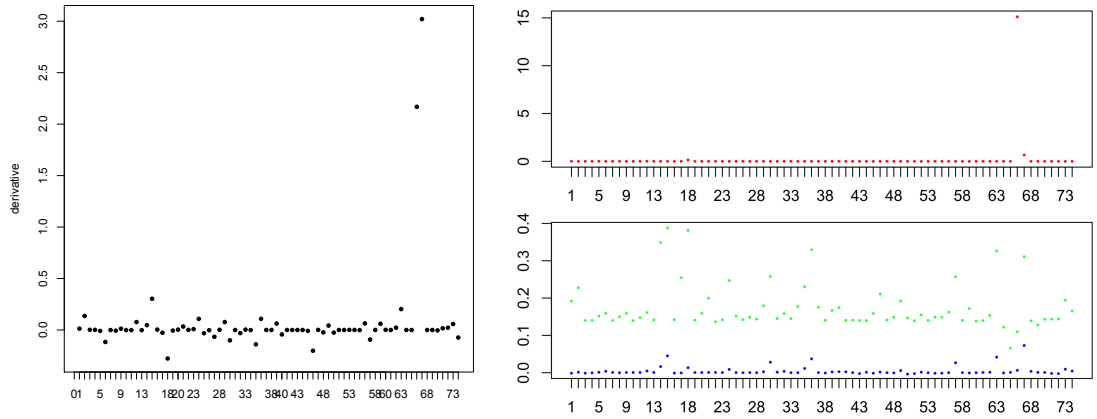

(a) Derivative

(b) $S^{loc}_{\{j\}}$ derivative (upper panel) and corresponding first order and total Sobol' indices (lower panel)

Figure 10: Derivative $\dfrac{\partial Y_{01}}{\partial X_i}$ (left), non dimensional derivative $S^{loc}_{\{j\}} = \dfrac{\mathrm{Var}(X_i)}{\mathrm{Var}(Y_{01})}\left(\dfrac{\partial Y_{01}}{\partial X_i}\right)^2$ (right, upper panel), and first order and total Sobol' indices (right, lower panel) as functions of the number of the parameter (x-axis). The derivatives are computed for $(x_1, \ldots, x_d) = (\mathrm{E}(X_1), \ldots, \mathrm{E}(X_d))$.

5.5. Computational costs

The relative computational costs of the different algorithms are displayed in Table 7, along with the estimated error related to the Sobol' indices (i.e. the half-length of the 95% bootstrap confidence interval). As mentioned earlier, the computation of total indices requires a number of model runs proportional to $d + 2$, which is much more than for the evaluation of only first- and second-order indices. Moreover, the estimation error is inversely proportional to $\sqrt{n}$, as is mainly the case in Monte Carlo methods, consistent with the rate of convergence in the central limit theorem. Note that other designs of experiments, such as quasi Monte Carlo methods, are not considered in this paper, since we do not assume any mathematical regularity in the underlying model. In the present case, given the order of magnitude of the indices, $n = 10^5$ appears to be a good compromise between accuracy and computational cost.

Estimation of Sobol' indices	`sobolSalt` n=10^5		`roalhs` n=10^3	`roalhs` n=10^4	`roalhs` n=10^5	`roalhs` n=10^6	`roalhs` q=227
	S1	ST	S1	S1	S1	S1	S2
Estimated Error							
maximum value	0.0076	0.0064	0.077	0.025	0.0077	0.0025	0.024
mean value	0.0065	0.0047	0.062	0.020	0.0064	0.0020	0.018
standard deviation	$2.0\,10^{-7}$	$2.3\,10^{-7}$	$2.7\,10^{-5}$	$3.4\,10^{-6}$	$5.7\,10^{-8}$	$3.2\,10^{-8}$	$2.7\,10^{-7}$
Number of evaluations	$7.6\,10^6$		$2\,10^3$	$2\,10^4$	$2\,10^5$	$2\,10^6$	$q^2 \simeq 10^5$

Table 7: Statistics (maximum and mean values, standard deviation) related to the estimated error over all 74 parameters, and number of model runs required for the estimation of the Sobol' indices.

6. Conclusion

The added value of SA is primarily to help scientists understanding the behavior of their models, and identifying their most influential parameters. Then, as a by-product in the context of model tuning, it helps focusing optimization effort on these few parameters (see for instance the two review papers by Oschlies (2006) and Dowd et al. (2014), and references herein, on data assimilation in the context of ocean biogeochemical models).

In the present work, a global sensitivity analysis based on Sobol' indices is presented in the context of a realistic ocean biogeochemical model. Without delving into complex physical interpretations, the aim of this study is

to demonstrate the potential interest of this systematic and mathematically sound approach for such applications. This method quantifies the influence of uncertain input parameters on an arbitrary number of output quantities of interest, either through their direct effect or through their mutual interactions. In the present study, which was performed with a full Monte Carlo method, thus avoiding any restrictive hypothesis on the effective dimension of the model or on its regularity, we started by computing first- and second-order indices. This highlighted on the one hand the strong influence of some input parameters and of some second-order interactions, and on the other that some higher order interactions were probably significant. Total Sobol' indices were thus computed, which provided complementary information. Note that total indices can also be a helpful source of information for constructing reduced models, since they identify parameters whose values could be frozen. These results were then compared to those derived using a local OAT gradient-based SA, where each parameter was varied individually around a point in parameter space corresponding to the average. It clearly illustrated the fact that a local SA can lead us to focus our attention on non globally relevant parameters and to neglect the influence of globally important ones. This comparison also brought out the strongly nonlinear character of the biogeochemical model considered here.

More generally, from a biogeochemical point of view, the methods described in this paper can provide a substantial help in the design of the models, in the tuning of their complexity, and in the understanding of their dependence to uncertainties in the parameters. It was shown indeed in our test application that the traditional sensitivity studies based on local methods can lead to misleading conclusions, and thus to a misunderstanding of the influence of every individual process on the key results of the simulations. Accounting for the nonlinear effects and for the interactions between the various processes is needed to decide what must be explicitly resolved by the model (and carefully tuned) and what can be roughly parameterized. Until recently, this ambition was very difficult to achieve. The take home message for further ocean biogeochemical research is that, due to the constant increase of computational resources, combined with recent advances in estimation procedures for the sensitivity measures, it is now possible to perform a global sensitivity analysis based on the computation of Sobol' indices. Large sets of input parameters can be considered and indices as expensive as total indices can be feasibly computed by taking advantage of grid computing environments which scale easily to high dimensional applications.

Appendix A. Estimation procedure for Sobol' indices

In this paper, we used a Monte Carlo based procedure for the estimation of Sobol' indices (Sobol', 1993), which we describe in detail below. Let us first introduce some notation. Let $\mathfrak{u}$ be a non-empty subset of $\{1, \dots d\}$. Let $\mathbf{X}^1 = (X_1^1, \dots, X_d^1)$ and $\mathbf{X}^2 = (X_1^2, \dots, X_d^2)$ be two independent copies of the input vector $\mathbf{X} = (X_1, \dots, X_d)$. Let $(\mathbf{X}^{1,i})_{i=1,\dots,n}$ be an *independent and identically distributed* (i.i.d.) sample of size n of vector $\mathbf{X}^1$ and $(\mathbf{X}^{2,i})_{i=1,\dots,n}$ be an i.i.d. sample of size n of vector $\mathbf{X}^2$. For any $\mathfrak{u} \subset \{1, \dots, d\}$, we define the d-dimensional vector $\mathbf{X}_\mathfrak{u} = (X_{\mathfrak{u},1}, \dots, X_{\mathfrak{u},d})$ in the following way: for any $j \in \mathfrak{u}$, $X_{\mathfrak{u},j}$ is equal to X_j^1, and for any $j \in \mathfrak{u}^c$, $X_{\mathfrak{u},j} = X_j^2$. The n-sample $(\mathbf{X}_\mathfrak{u}^i)_{i=1,\dots,n}$ is defined in a similar manner.

And we define the corresponding output variables:

$$Y = f(\mathbf{X}^1)\,,\ Y_\mathfrak{u} = f(\mathbf{X}_\mathfrak{u}) \text{ and } Y^i = f(\mathbf{X}^{1,i})\,,\ Y_\mathfrak{u}^i = f(\mathbf{X}_\mathfrak{u}^i). \tag{A.1}$$

It is possible to prove that $\mathrm{S}_\mathfrak{u}^{\text{closed}} = \dfrac{\mathrm{Cov}(Y, Y_\mathfrak{u})}{\mathrm{Var}[Y]}$ (see, e.g., Lemma 1.2 in Janon et al. (2014)). Based on the above formula, we propose the following estimator for $\mathrm{S}_\mathfrak{u}^{\text{closed}}$:

$$\hat{\mathrm{S}}_{\mathfrak{u},n}^{\text{closed}} = \frac{\dfrac{1}{n}\displaystyle\sum_{i=1}^n Y^i Y_\mathfrak{u}^i - \left(\dfrac{1}{n}\displaystyle\sum_{i=1}^n \frac{Y^i + Y_\mathfrak{u}^i}{2}\right)^2}{\dfrac{1}{n}\displaystyle\sum_{i=1}^n \frac{(Y^i)^2 + (Y_\mathfrak{u}^i)^2}{2} - \left(\dfrac{1}{n}\displaystyle\sum_{i=1}^n \frac{Y^i + Y_\mathfrak{u}^i}{2}\right)^2}\,. \tag{A.2}$$

This estimator was first introduced in Monod et al. (2006). Its asymptotic properties are stated in Janon et al. (2014, Propositions 2.2 and 2.5). See also Gamboa et al. (2016) for further asymptotic and non-asymptotic results.

Since $\mathrm{S}_{\{j\}} = \mathrm{S}_{\{j\}}^{\text{closed}}$ (see Eq. (5)), we therefore estimate $\mathrm{S}_{\{j\}}$ with $\hat{\mathrm{S}}_{\{j\},n} = \hat{\mathrm{S}}_{\{j\},n}^{\text{closed}}$.

Recall now the law of total variance which can be found, e.g., in (Weiss, 2006, pages 385-386):

$$\mathrm{Var}[Y] = \mathrm{Var}\big(\mathrm{E}(Y|\mathbf{X}_\mathfrak{u})\big) + \mathrm{E}\big(\mathrm{Var}(Y|\mathbf{X}_\mathfrak{u})\big)\,. \tag{A.3}$$

From the definition of total Sobol' indices, we can prove that:

$$\mathrm{S}_{\{j\}}^{\text{tot}} = \frac{\mathrm{E}\big(\mathrm{Var}(Y|X_{\{j\}^c})\big)}{\mathrm{Var}[Y]}\,. \tag{A.4}$$

From (A.3) and (A.4) we deduce $\mathrm{S}^{\mathrm{tot}}_{\{j\}} = 1 - \mathrm{S}^{\mathrm{closed}}_{\{j\}^c}$. We thus define the estimator of $\mathrm{S}^{\mathrm{tot}}_{\{j\}}$ as:

$$\hat{\mathrm{S}}^{\mathrm{tot}}_{\{j\},n} = 1 - \hat{\mathrm{S}}^{\mathrm{closed}}_{\{j\}^c,n}\,.$$

These estimators require a large number of model evaluations. Indeed, the estimation of all first-order indices actually requires $(d+1)n$ evaluations of the model: Y^i, $Y^i_{\{j\}}$, $i = 1, \ldots, n$, $j = 1, \ldots, d$. The estimation of all closed second-order indices requires $(\frac{d(d-1)}{2} + 1)n$ model evaluations of the model: Y^i, $Y^i_{\{j,k\}}$, $i = 1, \ldots, n$, $j \neq k = 1, \ldots, d$.

The Monte Carlo sample size n is directly related to the accuracy of the estimation via the rate of convergence in the central limit theorem, which is of order $\sqrt{n}$ (see Proposition 2.2 in Janon et al. (2014)).

To circumvent this linear or quadratic dependence of the cost (in terms of number of model evaluations) in the input space dimension d, the authors in Tissot and Prieur (2015) proposed a procedure based on replicated Latin Hypercube Sampling (LHS) (e.g. Lemieux, 2009) or replicated randomized orthogonal arrays to estimate all first-order or all closed second-order) Sobol' indices respectively. The ideas in Tissot and Prieur (2015) generalize some pioneer work in Mara and Rakoto Joseph (2008). We refer to Tissot and Prieur (2015) for a detailed description of the procedure, and a rigorous analysis of its asymptotic properties. In the present paper, we applied the replication procedure to estimate all first-order Sobol' indices in Subsection 5.1 and to estimate all closed second-order Sobol' indices in Subsection 5.2. More precisely, the replication procedure in Subsection 5.1 allows us to estimate all the first-order Sobol' indices with only two replicated d-dimensional LHS of size n, that is with only $2n$ model evaluations. The replication procedure in Subsection 5.2 allows to estimate all closed second-order Sobol' indices with only two replicated d-dimensional randomized orthogonal arrays of strength two and size n, that is with only $2n$ model evaluations. Due to constraints in the construction of orthogonal arrays of strength two, n must be chosen as q^2, with q a prime number greater or equal to $d-1$. Note that orthogonal arrays were introduced for the first time in Kishen (1942).

If higher order interactions are expected in the model (of any order greater or equal to three), one may be interested in estimating total Sobol' indices. The replication procedure does not adapt to the estimation of total Sobol' indices, mainly because of the constraints in the construction of orthogonal arrays of strength higher or equal to three. In Saltelli (2002), the authors

propose two different procedures, both based on combinatorial tricks: the first one allows the estimation of all first-order and total Sobol' indices with a cost of $(d+2)n$ model evaluations (see Theorem 1 in Saltelli (2002), the second one leads to a double estimate of all first-order, closed second-order and total Sobol' indices at a cost of $(2d+2)n$ model evaluations (see Theorem 2 in Saltelli (2002)). To our knowledge, the procedure in (Saltelli, 2002, Theorem 1) is the most competitive one if the estimation of total Sobol' indices is involved (see also Gilquin et al. (2017)). It is the one we have applied in Subsection 5.3.

Appendix B. Description of biogemical fluxes

The biogeochemical fluxes ($C_j \rightarrow C_i$) parameterized in MODECOGeL are summarized in Table B.8. Each flux depends on several parameters, which are indicated by referring to the parameter list in Table C.9 in Appendix C. To give an idea of the role of each parameter in MODECOGeL, the biogeochemical fluxes are organized into several categories using different colors:

- **Primary production (green)** is the growth of phytoplankton by photosynthesis. In Table B.8, this corresponds to all fluxes from nutrients (C_1, C_2) to phytoplankton (C_3, C_4, C_5). Parameters govern the maximum growth rate (1–3), and the dependence on nutrient concentrations (4–10), to solar irradiance (11-16), and to temperature (18–20).

- **Secondary production (blue)** is the growth of zooplankton by grazing of phytoplankton or by assimilation of bacteria and particulate organic matters. In Table B.8, this corresponds to all fluxes to zooplankton (C_6, C_7, C_8). Parameters govern the ingestion rate (28–33), the dependence on prey concentration (34–36), the efficiency according to the type of prey (37–43), and the fraction actually used for growth (55-59).

- **Mortality (red)** of living species, including a parameterization of predation by higher trophic levels. In Table B.8, this corresponds to all fluxes from phytoplankton or zooplankton or bacteria (C_3 to C_9) to particulate organic matter (C_{11} or C_{12}). Parameters govern mortality rates (44–50) and predation (51–53).

- **Exudation (magenta)** by phytoplankton. In Table B.8, this corresponds to all fluxes from phytoplankton (C_3, C_4, C_5) to dissolved organic nitrogen (C_{10}). Parameters are exudation rates (25–27).

- **Excretion (pink)** by zooplankton and bacteria. In Table B.8, this corresponds to all fluxes from zooplankton or bacteria (C_6 to C_9) to ammonium and dissolved organic nitrogen (C_2 and C_{10}). Parameters govern excretion rates (60–63), the dependence on temperature (64–67), the tradeoff between ammonium and dissolved organic matter (68), and the excreted fraction of predation (54).

- **Growth of bacteria (yellow)** from ammonium and dissolved organic matter. In Table B.8, this corresponds to all fluxes to bacteria (C_9). Parameters govern the growth rate (23–24).

- **Decomposition of particulate organic matter (orange)**. In Table B.8, this corresponds to all fluxes from particulate organic matter (C_{11} or C_{12}) to dissolved organic nitrogen (C_{10}). Parameters are decomposition rates (69–70).

- **Nitrification (brown)**. In Table B.8, this corresponds to the flux from ammonium (C_2) to nitrate (C_1). The parameter is the nitrification rate (72).

	Nutrients		Phytoplanktons			Zooplanktons			BAC	DON & POM		
	C_1	C_2	C_3	C_4	C_5	C_6	C_7	C_8	C_9	C_{10}	C_{11}	C_{12}
C_1			1,4,5, 11,14, 17,20	2,4,6, 12,15, 18,21	3,4,7, 13,16, 19,22							
C_2	72	72	1,8, 11,14, 17,20	2,9, 12,15, 18,21	3,10, 13,16, 19,22				23,24			
C_3			1,5,8, 11,14, 17,20, 25,44			28,31, 34,55				25	44	
C_4				2,6,9, 12,15, 18,21, 26,45			29,32, 35,56			26	45	
C_5					3,7,10, 13,16, 19,22, 27,46			30,33, 36,37, 57		27	46	
C_6						28,31, 34,47, 55,60, 64	29,32, 35,39, 56			60,64, 68	47	
C_7							29,32, 35,48, 56,61, 65	30,33, 36,40, 57		61,65, 68	48	
C_8								30,33, 36,49, 52,53, 54,57, 62,66		54,62, 66,68		49,51, 52,53
C_9						28,31, 34,38, 55	29,32, 35,56		23,24, 50,63, 67		50	
C_{10}									23,24			
C_{11}							29,32, 35,41, 58	30,33, 36,42, 59		69	69	
C_{12}								30,33, 36,43, 59		70		70

Table B.8: Biogeochemical fluxes from variable C_i (line i) to variable C_j (column j). Numbers in the boxes refer to parameter indices, given in Table C.9.

Appendix C. Model parameters

This table describes the different probability distributions chosen for input parameters.

Index	Name	Unit	Pdf	Mean	Std	Std/Mean
1	**PicP** max growth rate	t^{-1}	$\Gamma(25, 0.12)$	3.	0.6	20%
2	**NanP** max growth rate	t^{-1}	$\Gamma(25, 0.1)$	2.5	0.5	20%
3	**MicP** max growth rate	t^{-1}	$\Gamma(25, 0.08)$	2.	0.4	20%
4	dependence of **NO3** limitation to **NH4**	C^{-1}	$\Gamma(400, 0.00365)$	1.46	0.073	5%
5	**NO3** semisaturation for **PicP**	C	$\Gamma(4, 0.125)$	0.5	0.25	50%
6	**NO3** semisaturation for **NanP**	C	$\Gamma(4, 0.175)$	0.7	0.35	50%
7	**NO3** semisaturation for **MicP**	C	$\Gamma(4, 0.25)$	1.0	0.5	50%
8	**NH4** semisaturation for **PicP**	C	$\Gamma(4, 0.075)$	0.3	0.15	50%
9	**NH4** semisaturation for **NanP**	C	$\Gamma(4, 0.125)$	0.5	0.25	50%
10	**NH4** semisaturation for **MicP**	C	$\Gamma(4, 0.175)$	0.7	0.35	50%
11	optimal PAR for **PicP**	I	$\Gamma(25, 0.4)$	10.	2.	20%
12	optimal PAR for **NanP**	I	$\Gamma(25, 0.6)$	15.	3.	20%
13	optimal PAR for **MicP**	I	$\Gamma(25, 0.8)$	20.	4.	20%
14	variation of light limitation for **PicP**	–	$-\Gamma(4, 0.2)$	-0.8	0.4	50%
15	variation of light limitation for **NanP**	–	$-\Gamma(4, 0.175)$	-0.7	0.35	50%
16	variation of light limitation for **MicP**	–	$-\Gamma(4, 0.15)$	-0.6	0.3	50%
17	optimal temperature for **PicP**	T	$\mathcal{N}(15, 3^2)$	15.	3.	20%
18	optimal temperature for **NanP**	T	$\mathcal{N}(15, 3^2)$	15.	3.	20%
19	optimal temperature for **MicP**	T	$\mathcal{N}(16, 3.2^2)$	16.	3.2	20%
20	variation of temp. limitation for **PicP**	–	$-\Gamma(4, 0.125)$	-0.5	0.25	50%
21	variation of temp. limitation for **NanP**	–	$-\Gamma(4, 0.125)$	-0.5	0.25	50%
22	variation of temp. limitation for **MicP**	–	$-\Gamma(4, 0.1375)$	-0.55	0.275	50%
23	bacteria growth limitation	–	$\Gamma(4, 0.15)$	0.6	0.3	50%
24	semisaturation for **BAC** growth	C	$\Gamma(4, 0.125)$	0.5	0.25	50%
25	exudation ratio for **PicP**	–	$\Gamma(4, 0.015)$	0.06	0.03	50%
26	exudation ratio for **NanP**	–	$\Gamma(4, 0.0125)$	0.05	0.025	50%
27	exudation ratio for **MicP**	–	$\Gamma(4, 0.01)$	0.04	0.02	50%
28	max ingestion rate for **NanZ**	t^{-1}	$\Gamma(25, 0.12)$	3.	0.6	20%
29	max ingestion rate for **MicZ**	t^{-1}	$\Gamma(25, 0.08)$	2.	0.4	20%
30	max ingestion rate for **MesZ**	t^{-1}	$\Gamma(25, 0.06)$	1.5	0.3	20%
31	threshold ingestion for **NanZ**	C	$\Gamma(4, 0.0125)$	0.05	0.025	50%
32	threshold ingestion for **MicZ**	C	$\Gamma(4, 0.0075)$	0.03	0.015	50%
33	threshold ingestion for **MesZ**	C	$\Gamma(4, 0.0025)$	0.01	0.005	50%
34	semisaturation for ingestion by **NanZ**	C	$\Gamma(4, 0.125)$	0.5	0.25	50%
35	semisaturation for ingestion by **MicZ**	C	$\Gamma(4, 0.1875)$	0.75	0.375	50%
36	semisaturation for ingestion by **MesZ**	C	$\Gamma(4, 0.25)$	1.	0.5	50%
37	efficiency of **MesZ** on **MicP**	–	$\beta(4.2, 1.05)$	0.8	0.16	20%
38	efficiency of **NanZ** on **BAC**	–	$\beta(4.2, 1.05)$	0.8	0.16	20%
39	efficiency of **MicZ** on **NanZ**	–	$\beta(4.2, 1.05)$	0.8	0.16	20%
40	efficiency of **MesZ** on **MicZ**	–	$\beta(4.2, 1.05)$	0.8	0.16	20%
41	efficiency of **MicZ** on **MOP1**	–	$\beta(19.8, 79.2)$	0.2	0.04	20%
42	efficiency of **MesZ** on **MOP1**	–	$\beta(19.8, 79.2)$	0.2	0.04	20%
43	efficiency of **MesZ** on **MOP2**	–	$\beta(19.8, 79.2)$	0.2	0.04	20%
44	mortality rate for **PicP**	t^{-1}	$\Gamma(4, 0.015)$	0.06	0.03	50%
45	mortality rate for **NanP**	t^{-1}	$\Gamma(4, 0.0125)$	0.05	0.025	50%
46	mortality rate for **MicP**	t^{-1}	$\Gamma(4, 0.01)$	0.04	0.02	50%
47	mortality rate for **NanZ**	t^{-1}	$\Gamma(4, 0.015)$	0.06	0.03	50%

Index	Name	Unit	Pdf	Mean	Std	Std/Mean
48	mortality rate for **MicZ**	t^{-1}	$\Gamma(4, 0.0125)$	0.05	0.025	50%
49	mortality rate for **MesZ**	t^{-1}	$\Gamma(4, 0.0075)$	0.03	0.015	50%
50	mortality rate for **BAC**	t^{-1}	$\Gamma(4, 0.015)$	0.06	0.03	50%
51	threshold for predation	C	$\Gamma(4, 0.005)$	0.02	0.01	50%
52	maximum predation rate on **MesZ**	t^{-1}	$\Gamma(4, 0.25)$	1.	0.5	50%
53	semisaturation for predation on **MesZ**	C	$\Gamma(4, 0.25)$	1.	0.5	50%
54	excreted fraction of predation on **MesZ**	–	$\beta(2.33, 4.67)$	0.333	0.167	50%
55	fraction of grazing used for growth of **NanZ**	–	$\beta(4.2, 1.05)$	0.8	0.16	20%
56	fraction of grazing used for growth of **MicZ**	–	$\beta(4.2, 1.05)$	0.8	0.16	20%
57	fraction of grazing used for growth of **MesZ**	–	$\beta(4.2, 1.05)$	0.8	0.16	20%
58	fraction of POM used for growth of **MicZ**	–	$\beta(12, 12)$	0.5	0.1	20%
59	fraction of POM used for growth of **MesZ**	–	$\beta(12, 12)$	0.5	0.1	20%
60	excretion rate for **NanZ**	t^{-1}	$\Gamma(4, 0.0375)$	0.15	0.075	50%
61	excretion rate for **MicZ**	t^{-1}	$\Gamma(4, 0.025)$	0.1	0.05	50%
62	excretion rate for **MesZ**	t^{-1}	$\Gamma(4, 0.0125)$	0.05	0.025	50%
63	excretion rate for **BAC**	t^{-1}	$\Gamma(4, 0.0375)$	0.15	0.075	50%
64	temperature variation of excretion for **NanZ**	–	LogGamma	1.05	0.0525	5%
65	temperature variation of excretion for **MicZ**	–	LogGamma	1.05	0.0525	5%
66	temperature variation of excretion for **MesZ**	–	LogGamma	1.02	0.051	5%
67	temperature variation of excretion for **BAC**	–	LogGamma	1.04	0.052	5%
68	fraction of excretion as **DOM**	–	$\beta(2.75, 8.25)$	0.25	0.125	50%
69	POM1 decomposition rate	t^{-1}	$\Gamma(4, 0.01625)$	0.065	0.0325	50%
70	POM2 decomposition rate	t^{-1}	$\Gamma(4, 0.015)$	0.06	0.03	50%
71	sedimentation velocity for **MicP**	V	$\Gamma(4, 0.25)$	1.	0.5	50%
72	nitrification rate	t^{-1}	$\Gamma(4, 0.0075)$	0.03	0.015	50%
73	light attenuation coefficient in sea water	–	$\Gamma(25, 0.0016)$	0.04	0.008	20%
74	fraction of photosynthetically active radiation	–	$\Gamma(25, 0.02)$	0.5	0.1	20%

Table C.9: Model parameters X_i. Units are: time t in days, concentration C in mmolN/m^3, irradiance I in W/m^2, and velocity V in m/day. The notation $-\Gamma(.,.)$ means that the parameter is negative and that its opposite follows a $\Gamma(.,.)$ distribution.

References

G. Archer, A. Saltelli, and I. Sobol'. Sensitivity measures, ANOVA-like techniques and the use of bootstrap. *Journal of Statistical Computation and Simulation*, 58(2):99–120, 1997.

M. Baklouti, V. Faure, L. Pawlowski, and A. Sciandra. Investigation and sensitivity analysis of a mechanistic phytoplankton model implemented in a new modular numerical tool (eco3m) dedicated to biogeochemical modelling. *Progress in Oceanography*, 71(1):34–58, 2006.

M. Dowd, E. Jones, and J. Parslow. A statistical overview and perspectives on data assimilation for marine biogeochemical models. *Environmetrics*, 25(4):203–213, 2014.

J.-N. Druon and J. Le Fèvre. Sensitivity of a pelagic ecosystem model to variations of process parameters within a realistic range. *Journal of Marine Systems*, 19(1-3):1–26, 1999.

B. Efron and C. Stein. The jackknife estimate of variance. *The Annals of Statistics*, 9(3):586–596, 1981.

B. Faugeras, M. Lévy, L. Mémery, J. Verron, J. Blum, and I. Charpentier. Can biogeochemical fluxes be recovered from nitrate and chlorophyll data? a case study assimilating data in the northwestern Mediterranean sea at the JGOFS-DYFAMED station. *Journal of Marine Systems*, 40:99–125, 2003.

K. Fennel, M. Losch, J. Schröter, and M. Wenzel. Testing a marine ecosystem model: sensitivity analysis and parameter optimization. *Journal of Marine Systems*, 28(1-2):45–63, 2001.

F. Gamboa, A. Janon, T. Klein, A. Lagnoux, and C. Prieur. Statistical inference for Sobol pick freeze Monte Carlo method. *Statistics*, 50(4):881–902, 2016.

L. Gilquin, E. Arnaud, C. Prieur, and A. Janon. Making best use of permutations to compute sensitivity indices with replicated designs. working paper or preprint, June 2017. URL `https://hal.inria.fr/hal-01558915`.

W. F. Hoeffding. A class of statistics with asymptotically normal distributions. *Annals of Mathematical Statistics*, 19:293–325, 1948.

T. Homma and A. Saltelli. Importance measures in global sensitivity analysis of nonlinear models. *Reliability Engineering & System Safety*, 52(1):1–17, 1996.

A. Janon, T. Klein, A. Lagnoux, M. Nodet, and C. Prieur. Asymptotic normality and efficiency of two Sobol index estimators. *ESAIM: Probability and Statistics*, 18:342–364, 2014.

K. Kishen. On latin and hyper-graeco-latin cubes and hyper-cubes. *Current Science*, 11(3):98–99, 1942.

I. Kriest, A. Oschlies, and S. Khatiwala. Sensitivity analysis of simple global marine biogeochemical models. *Global Biogeochemical Cycles*, 26(2), 2012.

G. Lacroix. *Simulation de l'écosystème pélagique de la mer Ligure à l'aide d'un modèle unidimensionnel. Etude du bilan de matière et de la variabilité saisonnière, interannuelle et spatiale.* PhD thesis, Université Pierre et Marie Curie, Paris, France, 1998.

G. Lacroix and M. Grégoire. Revisited ecosystem model (MODECOGeL) of the Ligurian sea: seasonal and interannual variability due to atmospheric forcing. *J. Marine Syst.*, 37(4):229–258, 2002.

G. Lacroix and P. Nival. Influence of meteorological variability on primary production dynamics in the Ligurian Sea (NW Mediterranean sea) with a 1D hydrodynamic/biological model. *J. Marine Syst.*, 16(1-2):23–50, 1998.

C. Lemieux. *Monte Carlo and quasi-Monte Carlo sampling.* Springer Science & Business Media, 2009.

T. Mara and O. Rakoto Joseph. Comparison of some efficient methods to evaluate the main effect of computer model factors. *Journal of Statistical Computation and Simulation*, 78(2):167–178, 2008.

J.C. Marty and J. Chiavérini. Hydrological changes in the ligurian sea (nw mediterranean, dyfamed site) during 19952007 and biogeochemical consequences. *Biogeosciences*, 7(7):2117–2128, 2010.

H. Monod, C. Naud, and D. Makowski. Uncertainty and sensitivity analysis for crop models. In D. Wallach, D. Makowski, and J.W. Jones, editors, *Working with Dynamic Crop Models: Evaluation, Analysis, Parameterization, and Applications*, chapter 4, pages 55–99. Elsevier, 2006.

D.J. Morris, D.C. Speirs, A.I. Cameron, and M.R. Heath. Global sensitivity analysis of an end-to-end marine ecosystem model of the north sea: Factors affecting the biomass of fish and benthos. *Ecological Modelling*, 273:251–263, 2014.

M.D. Morris. Factorial sampling plans for preliminary computational experiments. *Technometrics*, 33(2):161–174, 1991.

J. C. J. Nihoul and S. Djenidi. Perspectives in three-dimensional modelling of the marine system. In J.C.J. Nihoul and B.M. Jamart, editors, *Three-Dimensional Models of Marine and Estuarine Dynamics*, pages 1–34. Elsevier, Amsterdam, 1987.

M. Omlin, R. Brun, and P. Reichert. Biogeochemical model of lake Zürich: sensitivity, identifiability and uncertainty analysis. *Ecological Modelling*, 141(1-3):105–123, 2001.

A. Oschlies. On the use of data assimilation in biogeochemical modelling. In *Ocean Weather Forecasting*, pages 525–547. Springer, 2006.

A. B. Owen. Orthogonal arrays for computer experiments, integration and visualization. *Statistica Sinica*, pages 439–452, 1992.

G. Pujol, B. Iooss, A. Janon, P. Lemaitre, L. Gilquin, L. Le Gratiet, T. Touati, B. Ramos, J. Fruth, and S. De Veiga. *Sensitivity: Global Sensitivity Analysis of Model Outputs*, 2017. R package version 1.15.0.

A. Saltelli. Making best use of model evaluations to compute sensitivity indices. *Computer Physics Communications*, 145(2):280–297, 2002.

A. Saltelli, K. Chan, and E.M. Scott. *Sensitivity analysis*. Wiley Series in Probability and Statistics. John Wiley & Sons, Ltd., Chichester, 2000.

S. Sankar, L. Polimene, L. Marin, N.N. Menon, A. Samuelsen, R. Pastres, and S. Ciavatta. Sensitivity of the simulated oxygen minimum zone to biogeochemical processes at an oligotrophic site in the arabian sea. *Ecological modelling*, 372:12–23, 2018.

M. Schartau, P. Wallhead, J. Hemmings, U. Löptien, I. Kriest, S. Krishna, B.A. Ward, T. Slawig, and A. Oschlies. Reviews and syntheses: parameter identification in marine planktonic ecosystem modelling. *Biogeosciences (BG)*, 14(6):1647–1701, 2017.

V. Scott, H. Kettle, and C. Merchant. Sensitivity analysis of an ocean carbon cycle model in the north Atlantic: an investigation of parameters affecting the air-sea CO2 flux, primary production and export of detritus. *Ocean Science*, 7(3):405–419, 2011.

I. Sobol'. Sensitivity analysis for nonlinear mathematical models. *Mathematical Modeling and Computational Experiment*, 1:407–414, 1993.

J.-Y. Tissot and C. Prieur. A randomized orthogonal array-based procedure for the estimation of first- and second-order Sobol' indices. *Journal of Statistical Computation and Simulation*, 85(7):1358–1381, 2015.

J.F. Tjiputra, D. Polzin, and A. Winguth. Assimilation of seasonal chlorophyll and nutrient data into an adjoint three-dimensional ocean carbon cycle model: sensitivity analysis and ecosystem parameter optimization. *Global biogeochemical cycles*, 21(1), 2007.

S. Wang, N. Flipo, and T. Romary. Time-dependent global sensitivity analysis of the c-rive biogeochemical model in contrasted hydrological and trophic contexts. *Water research*, 144:341–355, 2018.

N. A. Weiss. *A course in probability*. Addison-Wesley, Boston, MA, 2006. URL `http://cds.cern.ch/record/735662`.